

## Intracavity quartz-enhanced photoacoustic sensor

S. Borri, P. Patimisco, I. Galli, D. Mazzotti, G. Giusfredi, N. Akikusa, M. Yamanishi, G. Scamarcio, P. De Natale, and V. Spagnolo

Citation: [Applied Physics Letters](#) **104**, 091114 (2014); doi: 10.1063/1.4867268

View online: <http://dx.doi.org/10.1063/1.4867268>

View Table of Contents: <http://scitation.aip.org/content/aip/journal/apl/104/9?ver=pdfcov>

Published by the [AIP Publishing](#)

## Instruments for advanced science

### Gas Analysis



- dynamic measurement of reaction gas streams
- catalysis and thermal analysis
- molecular beam studies
- dissolved species probes
- fermentation, environmental and ecological studies

### Surface Science



- UHV TPD
- SIMS
- end point detection in ion beam etch
- elemental imaging - surface mapping

### Plasma Diagnostics



- plasma source characterization
- etch and deposition process reaction kinetic studies
- analysis of neutral and radical species

### Vacuum Analysis



- partial pressure measurement and control of process gases
- reactive sputter process control
- vacuum diagnostics
- vacuum coating process monitoring

contact Hiden Analytical for further details

**HIDEN**  
ANALYTICAL

[info@hideninc.com](mailto:info@hideninc.com)  
[www.HidenAnalytical.com](http://www.HidenAnalytical.com)

CLICK to view our product catalogue 



## Intracavity quartz-enhanced photoacoustic sensor

S. Borri,<sup>1,a)</sup> P. Patimisco,<sup>2</sup> I. Galli,<sup>1</sup> D. Mazzotti,<sup>1</sup> G. Giusfredi,<sup>1</sup> N. Akikusa,<sup>3</sup> M. Yamanishi,<sup>4</sup> G. Scamarcio,<sup>2</sup> P. De Natale,<sup>1</sup> and V. Spagnolo<sup>2</sup>

<sup>1</sup>CNR-INO UOS Sesto Fiorentino and LENS, via Carrara 1, 50019 Sesto Fiorentino FI, Italy

<sup>2</sup>CNR-IFN UOS Bari and Dipartimento Interateneo di Fisica, Università degli Studi di Bari e Politecnico di Bari, via Amendola 173, 70126 Bari BA, Italy

<sup>3</sup>Development Bureau Laser Device R&D Group, Hamamatsu Photonics KK, Shizuoka 434-8601, Japan

<sup>4</sup>Central Research Laboratories, Hamamatsu Photonics KK, Shizuoka 434-8601, Japan

(Received 4 December 2013; accepted 19 February 2014; published online 4 March 2014)

We report on a spectroscopic technique named intracavity quartz-enhanced photoacoustic spectroscopy (I-QEPAS) employed for sensitive trace-gas detection in the mid-infrared spectral region. It is based on a combination of QEPAS with a buildup optical cavity. The sensor includes a distributed feedback quantum cascade laser emitting at  $4.33\ \mu\text{m}$ . We achieved a laser optical power buildup factor of  $\sim 500$ , which corresponds to an intracavity laser power of  $\sim 0.75\ \text{W}$ .  $\text{CO}_2$  has been selected as the target molecule for the I-QEPAS demonstration. We achieved a detection sensitivity of 300 parts per trillion for 4 s integration time, corresponding to a noise equivalent absorption coefficient of  $1.4 \times 10^{-8}\ \text{cm}^{-1}$  and a normalized noise-equivalent absorption of  $3.2 \times 10^{-10}\ \text{W cm}^{-1}\ \text{Hz}^{-1/2}$ . © 2014 AIP Publishing LLC. [<http://dx.doi.org/10.1063/1.4867268>]

Trace gas detectors based on optical systems represent the best option for measuring tiny quantities of specific molecules, especially when fast on-line detection and high selectivity are needed. Since the advent of lasers, several spectroscopic methods have been developed for *in situ* trace-gas detection, leading in many cases to compact, reliable, and cost-effective sensors. Nowadays, optical gas sensing fills an important gap between low-cost sensors with inferior performance (pellistors, semiconductor gas sensors, or electrochemical devices) and high-end laboratory equipment, such as gas chromatographs.

Three main criteria drive the development of high-sensitivity optical sensors: (i) selection of optimal molecular transition in terms of absorption strength and absence of possible interfering gases; (ii) long optical absorption length and/or use of buildup optical cavity; and (iii) efficient spectroscopic detection schemes, e.g., frequency/wavelength modulation, balanced detection, photoacoustic spectroscopy (PAS), etc.

Among the cavity optical buildup methods, cavity-enhanced absorption spectroscopy (CEAS) and cavity ring-down (CRD) spectroscopy have demonstrated superior performances in terms of sensitivity levels.<sup>1,2</sup> CEAS makes use of coherent sources coupled to high-finesse optical resonators and takes advantage of the power buildup occurring inside the resonator. It allows to increase the detection capabilities with respect to standard direct-absorption spectroscopy by a factor which is usually proportional to the enhancement factor of the resonator. Similarly, high-finesse resonators with enhancement factors of several thousands have been used for CRD spectroscopy. They have recently allowed optical radiocarbon dating with a record sensitivity on  $^{14}\text{C}^{16}\text{O}_2$  detection in the parts-per-quadrillion (ppq) concentration range.<sup>2</sup> On the other hand, CRD spectrometers need stabilized sources, sophisticated locking loops, careful alignments, and vibrationless supports, therefore being often

confined to laboratory applications. Moreover, due to intracavity optical paths extended up to tens of kilometers, CRD deploys its full potential on low-pressure, diluted, and controlled gas samples.

Amid small-size and efficient spectroscopic sensors, PAS technique represents one of the best choices. Indeed, PAS is characterized by a compact, cost-effective, and robust architecture, which makes this technique ideal for *in-situ* gas sensing.<sup>3</sup> In particular, quartz-enhanced PAS (QEPAS)<sup>4</sup> combined with quantum cascade lasers (QCLs) has demonstrated sensitivities up to 50 parts per trillion (ppt) concentration levels in 1 s for  $\text{SF}_6$ , with a compact and robust apparatus.<sup>5,6</sup> Till now, the best performances have been obtained with mid-infrared (mid-IR) QCLs resonant with strong ro-vibrational molecular transitions although, very recently, high-sensitivity gas detection by a THz QCL has been demonstrated.<sup>7,8</sup> The QEPAS technique inverts the common photoacoustic approach<sup>3</sup> and accumulates the acoustic energy in a sharply resonant quartz tuning fork (QTF) with a very high quality factor, which acts as piezoelectric acoustic transducer.<sup>4</sup> QEPAS is characterized by a direct proportionality between the signal amplitude and the laser power available for gas excitation, so the higher the optical power focused between the QTF prongs, the lower the sensor detection limit.<sup>4</sup> Thus, combining optical build up and PAS detection may lead to the realization of optical sensors with unprecedented sensitivity. This method has been recently patented in very general configuration by Kachanov and Koulikov.<sup>9</sup> Moreover, a cavity-enhanced optical-feedback-assisted PAS sensors have been demonstrated for water vapor detection, achieving a noise-equivalent absorption coefficient of  $1.9 \times 10^{-10}\ \text{cm}^{-1}\ \text{Hz}^{-1/2}$ .<sup>10</sup>

In this paper, we report on the development of an innovative spectroscopic technique, which we named intracavity QEPAS (I-QEPAS). This technique can be considered as a merging of CEAS and QEPAS methods and exploits the merits of both of them. The enhancement of the light-matter

<sup>a)</sup>Electronic mail: simone.borri@ino.it

interaction path in a high-finesse buildup optical cavity corresponds to an effective interaction length of thousands of passes that can provide a proportional increase of the acoustic wave generation efficiency. Furthermore, the cavity behaves as a selective optical filter for the laser frequency, leading to more stable signals and better selectivity, once a proper locking between the laser frequency and the cavity mode is adopted. In addition, laser matching to the TEM<sub>00</sub> cavity mode provides an intracavity beam with an excellent spatial beam profile, thus effectively lowering the light-induced photoacoustic thermal noise.

CO<sub>2</sub> has been selected as the target gas for I-QEPAS proof-of-principle. CO<sub>2</sub> is the main product of combustion processes and of biological respiration both in vegetables and animals. Its monitoring has assumed a primary importance for global control of the environment and for industrial, medical, and geophysical purposes. PAS combined with a continuously tunable optical parametric oscillator emitting 20 mW of power at 4.23 μm has been used to detect CO<sub>2</sub> down to 7 ppb (parts per billion),<sup>11</sup> while mid-IR laser absorption spectroscopy combined with multipass cells have pulled the sensitivity limit down to 2.7 ppb.<sup>12</sup> The best commercial available CO<sub>2</sub> detector (Gäsera LP1), based on a micro electro-mechanical system (MEMS) cantilever sensor coupled with a laser interferometer, claims a detection limit of 3 ppb with 60 s integration time.

A schematic of the I-QEPAS sensor is shown in Figure 1. A bow-tie optical resonator with a finesse exceeding 1500 has been specifically designed for coupling to a QTF detection system. The laser source used in this work is a room-temperature continuous-wave distributed-feedback QCL (provided by Hamamatsu Photonics) emitting at 4.33 μm wavelength.

It has a threshold current of 650 mA at 283 K operating temperature and provides up to 10 mW optical power at 800 mA driving current. A home-made low-noise current driver allows to keep the laser linewidth within ~1 MHz (FWHM) over tens of ms timescales.<sup>13</sup> The QCL is equipped with a field effect transistor (FET) controller, through which fast modulations (exceeding tens of MHz) can be applied directly to the laser chip. Slow (<1 kHz) modulations for

mode-hop-free frequency tuning can be obtained by applying voltage signals to a modulation input of the current driver. The laser radiation is collimated by a 5-mm focal length ZnSe aspheric lens. By means of a polarizing beam splitter, a small fraction of the emitted power (~10%) is sent to a reference cell filled with pure CO<sub>2</sub> and detected by a HgCdTe photodiode. The rest of the beam, transmitted by the beam splitter, is coupled to the optical resonator for power buildup. A 100-mm focal length CaF<sub>2</sub> plano-convex lens is used for mode matching with the cavity TEM<sub>00</sub> mode. A quarter-wave retardation plate is placed between the beam splitter and the mode-matching lens to avoid optical feedback towards the laser. The high-finesse optical resonator consists of four 0.5-in. diameter mirrors (two plane and two concave with 30 mm radius of curvature). All mirrors are coated with dielectric layers yielding a reflectivity  $R = 99.9\%$  at the target wavelength. A travelling-wave bow-tie resonator design has been chosen, with the mirrors tilted by 10° with respect to the incident beam, in order to avoid strong feedback onto the QCL induced by any radiation retro-reflected from the input mirror. The total cavity length is  $L = 174$  mm, corresponding to a free spectral range ( $FSR = c/L$ ) of 1.725 GHz. One of the plane mirrors is mounted on a piezoelectric transducer (PZT) which allows a fine tuning of the cavity length in a range of ~10 μm. The measured width of the cavity modes (under vacuum) is  $\Delta\nu = 1.15$  MHz (FWHM), corresponding to a finesse  $F = FSR/\Delta\nu = 1505$  and an enhancement factor  $G = F/\pi = 480$ , in good agreement with the values estimated by taking into account the power losses due to the mirrors transmissivity ( $F = 2\pi/(\text{total losses per round trip}) = 1570$ ,  $G = 500$ ). The achieved mode matching was ~50% of incident power, extracted by measuring the optical power reflected by the input mirror. The intracavity optical power is thus enhanced by a factor ~250 with respect to the incident one.

The resonator is placed inside a custom-designed metallic vacuum chamber equipped with anti-reflection-coated CaF<sub>2</sub> windows and with input/output valves for gas filling. An InSb photodiode is placed after the output coupler of the cavity and detects the exiting radiation. The cavity is designed to produce a 60 μm waist (radius at 1/e<sup>2</sup> intensity) between the two spherical mirrors (astigmatic distortions can be neglected). At the focus point, we placed the QTF mounted on an xyz translator. All the beam power passed between the prongs of the fork (spaced by 300 μm) without hitting it. Indeed, this is a mandatory condition in order to not degrade the finesse and to reduce thermal noise and spurious background on the photoacoustic signal.<sup>14,15</sup> A custom-built control electronics unit (CEU) is used to measure the electrical parameters of the QTF (the dynamical resistance, the quality factor  $Q$ , and the resonant frequency  $f_0$ ). The measured QTF resonance frequency is  $f_0 \sim 32\,772$  Hz and the quality factor  $Q$  exceeds 32 000 at the operating pressure conditions (~50 mbar). An electric resistance of 42.1 kΩ was measured, leading to a QTF thermal noise of 11.6 μV.<sup>4</sup>

For spectral scans, the QCL injected current was linearly tuned around the selected molecular transition by applying a slow voltage ramp to the current driver. A home-made electronic control loop was used to lock the resonant frequency of the cavity to the laser frequency for each step of the slow

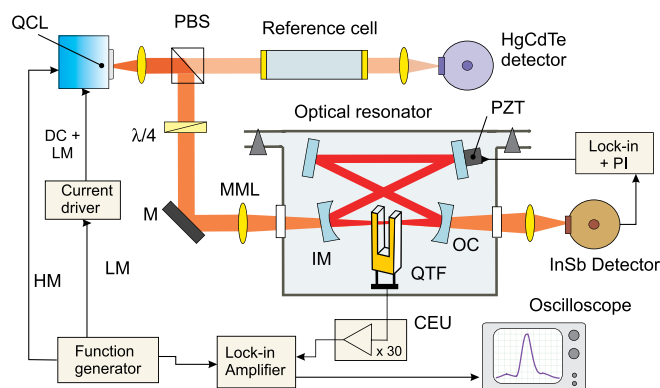


FIG. 1. Schematic of the I-QEPAS setup. PBS: polarizing beam splitter;  $\lambda/4$ : quarter-wave plate; M: mirror; MML: mode-matching lens; IM: input mirror; OC: output coupler; PI: proportional-integral controller; LM: low-frequency modulation (linear ramp); HM: high-frequency modulation (sinusoidal dither); CEU: control electronics unit. The whole system is assembled on a 60 × 30 cm breadboard, with large room for further shrinking.

linear scan. The laser current was sinusoidally modulated at the frequency  $f_0/2$  through the FET, with a modulation depth  $\Delta\nu$  large enough to scan completely the resonance of the cavity during each half period. The optimal value  $\Delta\nu \sim 10$  MHz (peak-to-peak) was obtained by measuring the I-QEPAS peak signal as a function of the laser modulation depth at the operating pressure conditions. The signal generated by the InSb detector was processed by a lock-in amplifier; its output (error signal) was processed by a proportional-integral operational amplifier module and used for closing a locking loop acting on the PZT tuning the cavity length. The locking loop, as well as the PZT response, was not fast enough to follow the fast dither at  $f_0/2$ . Its task was to maintain the optical cavity resonant with the laser frequency at the center of the fast dither, forcing the resonator to scan across the absorption line following the slow linear ramp applied to the QCL. The cavity consequently acts as a mechanical chopper at frequency  $f_0$  for the infrared light radiation, thus making our sensor to work in amplitude modulation (AM) regime. The signal from the QTF was finally demodulated at the frequency  $f_0$  by another lock-in amplifier.

The I-QEPAS sensor was tested on the  $(00^01)-(00^00)$  P(42) ro-vibrational transition of  $\text{CO}_2$ , centered at  $2311.105\text{ cm}^{-1}$ , having a linestrength  $S = 4.749 \times 10^{-19}\text{ cm/mol}$ .<sup>16</sup> Due to absorption from ambient  $\text{CO}_2$  in air, we observed a significant attenuation of the laser beam along its path ( $\sim 30\text{ cm}$ ) before entering the cavity. Therefore, the available power at the center of the absorption line was reduced to 3 mW (corresponding to an intracavity power  $\sim 0.75\text{ W}$ ). The acquired signal is composed by three main contributions: a flat background, due to acoustic signal from laser absorption by the resonator windows and mirrors; a Lorentzian-shaped broad contribution due to ambient  $\text{CO}_2$  absorption in the optical path outside the cavity; and the I-QEPAS signal due to the  $\text{CO}_2$  inside the cavity. In order to determine the two background contributions, we have performed I-QEPAS measurements, in spectral scan mode, with pure nitrogen in the optical cavity. We verified that the overall background signal could be easily fitted by a Lorentzian function (4.72 GHz FWHM), plus a flat offset. We used the same post-process procedure to subtract the background components from the acquired I-QEPAS spectra. The optimal sensor operating conditions were found to occur at a modulation amplitude of 70 mV peak-to-peak ( $\Delta\nu \sim 10$  MHz) and a gas pressure of 50 mbar. In Figure 2, a spectral scan of the P(42) line for a 50 ppb  $\text{CO}_2:\text{N}_2$  mixture (5 s sampling time, lock-in set to 1 s time constant) is shown before (a) and after (b) background removal. As expected, the I-QEPAS spectral signal does not exhibit a 2nd-derivative-like shape, but has the typical absorption profile of pure AM detection. Considering the noise fluctuations and the I-QEPAS peak signal, we can roughly estimate a  $1\text{-}\sigma$  detection limit of  $\sim 1$  ppb at 5 s integration time.

A comparison between the standard single-pass QEPAS signal obtained under the same operating conditions, in terms of pressure and incident laser power, shows an improvement by a factor  $\sim 250$ , in very good agreement with the expected power enhancement factor.

The response of the sensor was investigated by plotting the I-QEPAS peak signal as a function of the  $\text{CO}_2$  concentration

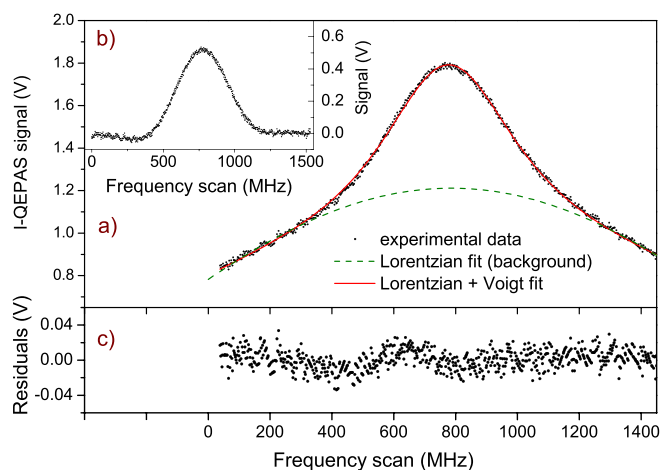


FIG. 2. I-QEPAS spectral scan of a 50 ppb  $\text{CO}_2:\text{N}_2$  gas sample (50 mbar pressure) before (a) and after (b) background removal. The overall spectral fit (solid red line) of the experimental data consists of two functions: a Lorentzian function + flat offset for the background (dashed green curve) and a Voigt function for the effective I-QEPAS signal. (c) Residuals plot.

between 0 ppb (pure  $\text{N}_2$ ) and 860 ppb. The results are shown in Figure 3. The horizontal error bars take into account the uncertainty on the concentration values, which we estimate in about 5% for dilutions (uncertainty on pressure gauge) and in 2% for the certified samples (data from the gas mixture provider). All the experimental data were normalized to the cavity finesse in vacuum, in order to take into account the decreasing enhancement factor (and thus the intracavity power) with increasing internal absorption losses given by higher  $\text{CO}_2$  concentrations.

In order to determine the best achievable sensitivity and long-term drifts of the sensor, we performed an Allan deviation analysis<sup>17</sup> of a 90-min acquisition of the signal (150 ms sampling time with 30 ms lock-in time constant) measured for 50 mbar of pure  $\text{N}_2$  in locking conditions. The Allan deviation is shown in Figure 4.

From this analysis, we can extract a sensitivity of 300 ppt at  $\sim 20\text{ s}$  integration time (i.e., 4 s lock-in time constant, with a 0.017 Hz equivalent noise bandwidth considering a 12 dB/octave lock-in filter slope). The corresponding minimum absorption coefficient is  $\alpha_{\min} = 1.4 \times 10^{-8}\text{ cm}^{-1}$

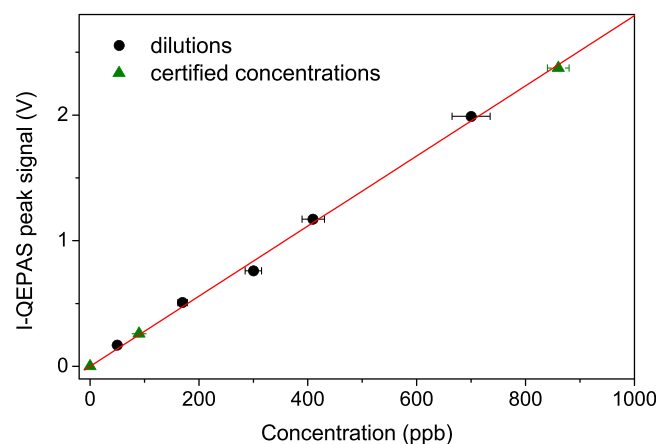


FIG. 3. I-QEPAS peak signal (1-s lock-in time constant) vs  $\text{CO}_2$  concentration. Solid red line: best fit of the data (intercept forced to zero). The adjusted R-square results 0.997.

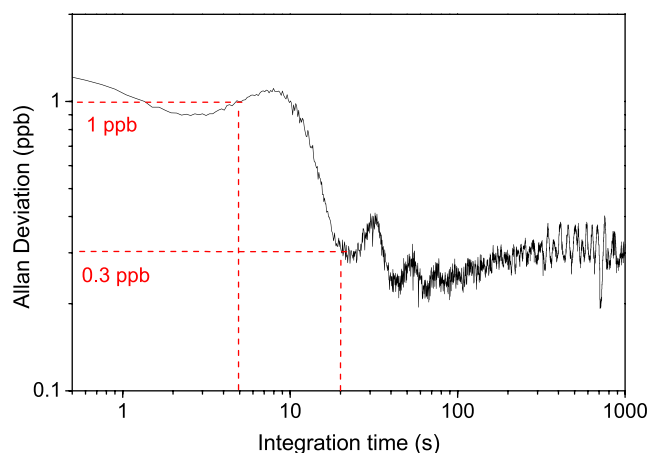


FIG. 4. Allan deviation of the I-QEPAS signal as a function of the acquisition time. The oscillations can be ascribed to the laser-resonator locking loop and to mechanical oscillations of the QTF module.

and the normalized noise-equivalent absorption (NNEA) is  $3.2 \times 10^{-10} \text{ W cm}^{-1} \text{ Hz}^{-1/2}$ . With these values, our spectrometer results to be over one order of magnitude more sensitive than all reported QEPAS-based sensors for  $\text{CO}_2$  detection (sensitivities of 18 ppm (Ref. 18) and NNEA of  $4 \times 10^{-9} \text{ W cm}^{-1} \text{ Hz}^{-1/2}$  (Ref. 19)). Its sensitivity is similar to the best cantilever-based sensors reported in literature,<sup>20,21</sup> with the advantage of a simpler, more cost-effective, and robust detection module. However, the I-QEPAS technique can potentially achieve even much lower sensitivity levels. In fact, our system makes use of a bare QTF as acoustic detection module and the sensor performances can be improved by at least one order of magnitude by coupling the QTF with an acoustic organ-pipe-type micro-resonator.<sup>22</sup> Moreover, the background signal due to windows and laser absorption by ambient  $\text{CO}_2$  in the optical path outside the cavity can be removed by placing the laser source inside a pressure-controlled box. It is worth noting that the photoacoustic signal is affected by the molecular vibrational-translational (V-T) relaxation rate and  $\text{CO}_2$  is characterized by a slow rate. Therefore, adding to the gas mixture, a relaxation promoter such as  $\text{SF}_6$  or water vapor may further enhance the I-QEPAS signal.<sup>23</sup>

This work was financially supported by the Italian Ministry for University and Research through the Italian national Project Nos. PON01\_02238, PON02\_00675, PON02\_00576, by the project “Active Ageing@home”

within the National Technological Cluster (CTN) venture in the PON-2013-FESR framework, and by the Laserlab-Europe consortium within the Joint Research Activity 2012-2015 JRA4: EURO-LITE.

- <sup>1</sup>P. Cancio, I. Galli, S. Bartalini, G. Giusfredi, D. Mazzotti, and P. De Natale, in *Cavity-Enhanced Spectroscopy and Sensing*, Springer Series in Optical Sciences Vol. 179, edited by G. Gagliardi and H.-P. Looks (Springer, 2014), pp. 143–162.
- <sup>2</sup>I. Galli, S. Bartalini, S. Borri, P. Cancio, D. Mazzotti, P. De Natale, and G. Giusfredi, *Phys. Rev. Lett.* **107**, 270802 (2011).
- <sup>3</sup>A. Elia, P. M. Lugarà, C. Di Franco, and V. Spagnolo, *Sensors* **9**, 9616 (2009).
- <sup>4</sup>A. A. Kosterev, F. K. Tittel, D. V. Serebryakov, A. L. Malinovsky, and I. V. Morozov, *Rev. Sci. Instrum.* **76**, 043105 (2005).
- <sup>5</sup>V. Spagnolo, P. Patimisco, S. Borri, G. Scamarcio, B. E. Bernacki, and J. Kriesel, *Opt. Lett.* **37**, 4461 (2012).
- <sup>6</sup>V. Spagnolo, P. Patimisco, S. Borri, G. Scamarcio, B. E. Bernacki, and J. Kriesel, *Appl. Phys. B: Lasers Opt.* **112**, 25 (2013).
- <sup>7</sup>S. Borri, P. Patimisco, A. Sampaolo, M. S. Vitiello, H. E. Beere, D. A. Ritchie, G. Scamarcio, and V. Spagnolo, *Appl. Phys. Lett.* **103**, 021105 (2013).
- <sup>8</sup>P. Patimisco, S. Borri, A. Sampaolo, M. S. Vitiello, H. E. Beere, D. A. Ritchie, G. Scamarcio, and V. Spagnolo, “A quartz enhanced photoacoustic gas sensor based on a custom tuning fork and a terahertz quantum cascade laser,” *Analyst* (published online).
- <sup>9</sup>A. Kachanov and S. Koulikov, U.S. patent 8,379,206 B2 (19 February 2013).
- <sup>10</sup>A. Kachanov, S. Koulikov, and F. K. Tittel, *Appl. Phys. B: Lasers Opt.* **110**, 47 (2013).
- <sup>11</sup>M. M. J. W. van Herpen, A. K. Y. Ngai, S. E. Bisson, J. H. P. Hackstein, E. J. Woltering, and F. J. M. Harren, *Appl. Phys. B: Lasers Opt.* **82**, 665 (2006).
- <sup>12</sup>A. Manninen, B. Tuzson, H. Looser, Y. Bonetti, and L. Emmenegger, *Appl. Phys. B: Lasers Opt.* **109**, 461 (2012).
- <sup>13</sup>S. Bartalini, S. Borri, I. Galli, G. Giusfredi, D. Mazzotti, T. Edamura, N. Akikusa, M. Yamanishi, and P. De Natale, *Opt. Express* **19**, 17996 (2011).
- <sup>14</sup>V. Spagnolo, A. A. Kosterev, L. Dong, R. Lewicki, and F. K. Tittel, *Appl. Phys. B: Lasers Opt.* **100**, 125 (2010).
- <sup>15</sup>L. Dong, V. Spagnolo, R. Lewicki, and F. K. Tittel, *Opt. Express* **19**, 24037 (2011).
- <sup>16</sup>L. S. Rothman, I. E. Gordon, Y. Babikov, A. Barbe, D. C. Benner, P. F. Bernath, M. Birk, L. Bizzocchi, V. Boudon, L. R. Brown et al., *J. Quant. Spectrosc. Radiat. Transfer* **130**, 4 (2013).
- <sup>17</sup>D. W. Allan, *Proc. IEEE* **54**, 221 (1966).
- <sup>18</sup>R. Lewicki, G. Wysocki, A. A. Kosterev, and F. K. Tittel, *Appl. Phys. B: Lasers Opt.* **87**, 157 (2007).
- <sup>19</sup>A. A. Kosterev, L. Dong, D. Thomazy, F. K. Tittel, and S. Overby, *Appl. Phys. B: Lasers Opt.* **101**, 649 (2010).
- <sup>20</sup>T. Laurila, H. Cattaneo, V. Koskinen, J. Kauppinen, and R. Hernberg, *Opt. Express* **13**, 2453 (2005).
- <sup>21</sup>V. Koskinen, J. Fonsen, K. Roth, and J. Kauppinen, *Appl. Phys. B: Lasers Opt.* **86**, 451 (2007).
- <sup>22</sup>L. Dong, A. A. Kosterev, D. Thomazy, and F. K. Tittel, *Appl. Phys. B: Lasers Opt.* **100**, 627 (2010).
- <sup>23</sup>G. Wysocki, A. A. Kosterev, and F. K. Tittel, *Appl. Phys. B: Lasers Opt.* **85**, 301 (2006).